

ORIGINAL ARTICLE

Health, Nutrition, and Food

Antioxidant, anti-inflammatory, hypoglycemic, and anti-hyperglycemic activity of chickpea protein hydrolysates evaluated in BALB-c mice

Alicia Navarro-Leyva | Gabriela López-Angulo | Francisco Delgado-Vargas | José Ángel López-Valenzuela 

Facultad de Ciencias Químico Biológicas,
Universidad Autónoma de Sinaloa,
Ciudad Universitaria, Culiacán, Sinaloa,
México

Correspondence

José Ángel López-Valenzuela, Facultad de
Ciencias Químico Biológicas, Av.
Américas y Josefa Ortiz S/N, Culiacán,
Sinaloa, 80010, México.
Email: jalopezvla@uas.edu.mx

Funding information

Universidad Autónoma de Sinaloa,
Grant/Award Numbers: PROFAPI,
PRO-A7-021

Abstract: Chickpea (ICC3761) protein hydrolysates have shown high in vitro antioxidant activity (AoxA) and antidiabetic potential. The aim of this study was to evaluate the in vivo activities (i.e., antioxidant, anti-inflammatory, hypoglycemic, and anti-hyperglycemic) of chickpea albumin hydrolysates (CAH) obtained with alcalase and pepsin-pancreatin (fractions ≤ 10 kDa). The CAH were analyzed for degree of hydrolysis (DH), electrophoretic and chromatographic profiles, and in vitro AoxA (2,2'-azino-bis(3-ethylbenzothiazolin)-6-sulfonic acid [ABTS], 2,2-diphenyl-1-picrylhydrazyl [DPPH]). They were also evaluated for AoxA, anti-inflammatory and hypo- and anti-hyperglycemic activities in BALB-c mice. The DH was 20% for the alcalase CAH and 50% for the pepsin-pancreatin CAH, while the AoxA by ABTS (1 mg/mL) was 64.8% and 64.9% and by DPPH (5 mg/mL) was 48.0% and 31.1%. In the in vivo AoxA assay, mice of non-damaged control and those treated with both CAH showed similar alkaline phosphatase values, control and pepsin-pancreatin treated groups had similar malondialdehyde levels, while treated and non-damaged control groups had higher glutathione levels than the damaged control. Liver histopathology revealed that the pepsin-pancreatin CAH mitigated most of the pathological changes associated with the induced oxidative damage. Both CAH (2 mg/ear) reduced croton oil-induced ear edema in mice. The α -glucosidase inhibition of CAH (100 mg/mL) was 31.1% (alcalase) and 52.4% (pepsin-pancreatin). Mice treated with alcalase CAH (100 mg/mL) and glibenclamide exhibited similar hypoglycemic activities, whereas only those treated with the pepsin-pancreatin CAH (200 mg/kg body weight) showed anti-hyperglycemic activity. The results indicate that CAH can be used as a source of bioactive peptides with antioxidant, anti-inflammatory, hypoglycemic, and anti-hyperglycemic activities.

KEYWORDS

antidiabetic, bioactive peptides

Alicia Navarro-Leyva and Gabriela López-Angulo contributed equally to this work.

1 | INTRODUCTION

Chickpea (*Cicer arietinum* L.) is the third most widely produced legume worldwide (FAOSTAT, 2022) and an important source of proteins (15%–30%) for human nutrition. These proteins are also good sources of bioactive peptides (2–20 residues), typically released by enzymatic digestion. The peptides produced have several health-promoting properties such as antioxidant, anti-inflammatory, angiotensin converting enzyme (ACE) inhibitory activity, antitumor and antiproliferative effects, and potential antidiabetic properties (Acevedo-Martínez & Gonzalez de Mejia, 2021; Chavez-Ontiveros et al., 2022; Kou et al., 2013; Quintero-Soto et al., 2021; Xue et al., 2015). However, the in vivo effects of chickpea hydrolysates have been demonstrated mainly for the anti-hypertensive activity in spontaneously hypertensive rats (Chavez-Ontiveros et al., 2022).

Quintero-Soto et al. (2021) evaluated the antioxidant and antidiabetic potential of chickpea hydrolysates prepared with alcalase from the albumin and globulin fractions of 18 genotypes. The peptides derived from the albumin fraction showed the highest antioxidant activity (AoxA; 2,2'-azino-bis(3-ethylbenzothiazolin)-6-sulfonic acid [ABTS] and 2,2-diphenyl-1-picrylhydrazyl [DPPH]) and the greatest inhibition of enzymes related to diabetes (α -amylase, α -glucosidase, and dipeptidyl peptidase-4 [DPP4]). In addition, other chickpea protein hydrolysates obtained with pepsin-pancreatin and bromelain also showed good inhibition of DPP4 (Acevedo-Martínez & Gonzalez de Mejia, 2021). However, the evaluation of the hypoglycemic activity of protein hydrolysates in vivo has only been reported for other legumes so far.

Mojica et al. (2017) evaluated the hypoglycemic potential of a black bean protein hydrolysate obtained using alcalase. The hydrolysate was administered to healthy male Wistar rats (50 mg/kg body weight, BW), and it reduced the postprandial glucose levels. Also, it lowered the glucose levels in a hyperglycemic rat model at doses of 150 and 200 mg/kg BW/day. Furthermore, the hydrolysate decreased the levels of intracellular reactive oxygen species and prevented the increase of hepatic markers. Similar anti-hyperglycemic activities were observed in normoglycemic Wistar rats treated with alcalase and pepsin-pancreatin hydrolysates from other common bean varieties (Nuñez-Aragón et al., 2019; Valencia-Mejía et al., 2019). Furthermore, a pepsin-pancreatin hydrolysate from a common bean showed hypoglycemic activity in normal Institute of Cancer Research (ICR) mice (Valencia-Mejía et al., 2019).

Inflammation encompasses oxidative stress and is associated with health disorders such as diabetes and cardiovascular diseases. Milan-Noris et al. (2018) demon-

strated the anti-inflammatory potential of chickpea protein digests (α -amylase-pepsin-pancreatin) in lipopolysaccharide (LPS)-induced RAW264.7 macrophages. The inhibition of nitric oxide (NO) production (Half-maximal inhibitory concentration, IC₅₀) by the protein digests from germinated chickpea (2.01 mg/mL) was more effective than that from cooked samples (3.55 mg/mL). Dehiba et al. (2021) evaluated the antioxidant and anti-inflammatory effects of chickpea protein hydrolysates (1 g/kg BW) in cholesterol-fed rats, which showed reduced serum levels of hydroperoxide, malondialdehyde (MDA), C-reactive protein, uric acid, and albumin.

The information about the in vivo evaluation of the potential health-promoting properties of chickpea hydrolysates is limited. Therefore, the aim of this research was to evaluate the antioxidant, anti-inflammatory, hypoglycemic, and anti-hyperglycemic activities of alcalase and pepsin-pancreatin chickpea albumin hydrolysates (CAH) in BALB-c mice.

2 | MATERIALS AND METHODS

2.1 | Biological material

A desi-type black chickpea (*C. arietinum* L.) genotype (ICC3761) from the International Crops Research Institute for the Semi-Arid Tropics was used. It was grown at the experimental field of the National Institute of Forestry, Agriculture and Livestock Research in Culiacan, Sinaloa, Mexico, as described by Chavez-Ontiveros et al. (2020). Mature seeds were ground (Retsch MM400, Haan, Germany) and passed through a 60-mesh sieve.

2.2 | Animals

BALB-c mice (BIOINVERT SA de CV, Ecatepec de Morelos, Mexico) were used for the in vivo assays. The animals were housed in acrylic boxes in a temperature-controlled room ($24 \pm 1^\circ\text{C}$) with 12-h light/dark cycles and had free access to drinking water and rodent feed (Nutricubes, Purina, St. Louis, MO, USA). The research was conducted following the Mexican Official Standard NOM062-ZOO-1999.

2.3 | Extraction and quantification of albumins

The albumin fraction was extracted according to Ortiz-Martinez et al. (2017) with modifications in the ratio of flour/hexane and the extraction time. About 20 g of flour

was first defatted with 400 mL of hexane. The recovered pellet was mixed with 400 mL of sterile deionized water (H₂O, pH 8.0), stirred for 4 h at 20°C, centrifuged (15,000 × g, 20 min, 25°C; 5804R, Eppendorf, Hamburg, Germany), and the supernatant was lyophilized (25EL, Vir-Tis Co., Gardiner, NY, USA). The dried albumin fraction was washed sequentially with methanol (200 mL) and acetone (200 mL). The concentration was determined using the bicinchoninic acid assay (Brown et al., 1989).

2.4 | Preparation of hydrolysates

2.4.1 | Hydrolysis with alcalase

Albumins (1 g) were resuspended in 10 mL of water (pH 8.0) and heated in a water bath at 80°C for 5 min. The sample was then cooled down to 50°C and mixed with the alcalase enzyme (0.3 AU/g protein; P4860, Sigma-Aldrich, St. Louis, MO, USA). The hydrolysis was carried out for 180 min at 50°C while maintaining a constant pH of 8.0 with 5 N sodium hydroxide (NaOH). The sample was incubated at 80°C for 20 min to inactivate the enzyme and then left to stand at room temperature for 10 min. The sample was centrifuged (5000 × g, 20 min, 4°C; 5804R, Eppendorf) and the recovered supernatant was filtered (0.45 µm; PVDF membrane, HPLC certified, Pall Corp., Port Washington, NY, USA). Finally, the filtrate was passed through 10 kDa molecular weight (MW) cut-off tubes to remove non-hydrolyzed protein debris. The recovered filtrate was lyophilized and stored at -20°C until further use. The yield (%) was calculated by dividing the weight of the hydrolysate by the protein weight and then multiplying by 100. The degree of hydrolysis (DH) was calculated as follows: $DH (\%) = (h/h_{tot}) 100$; where h is the concentration of amino groups formed during hydrolysis in mmol/g protein and h_{tot} was assumed to be 7.22 mmol/g protein according to Kou et al. (2013) and Adler-Nissen (1979).

2.4.2 | Hydrolysis with pepsin-pancreatin

Sequential hydrolysis with pepsin and pancreatin was performed according to Acevedo-Martínez & Gonzalez de Mejia (2021) with some modifications. An enzyme-substrate ratio of 1:20 was used for both pepsin (3200 U/mL; P6887, Sigma-Aldrich) and pancreatin (8 × USP; P7545, Sigma-Aldrich). First, 1 g of albumin was mixed with pepsin solution (20 mL of 0.01 M hydrochloric acid [HCl], pepsin; pH 2) and stirred at 37°C for 90 min. Subsequently, the pH was adjusted to 8.0 with 1 M NaOH, the pancreatin solution (7.5 mL phosphate buffer, pancreatin; pH 8) was added, and the mixture was stirred for 90 min

at 37°C. The enzymes were inactivated at 80°C for 20 min, followed by cooling at room temperature for 10 min. The sample was centrifuged (5000 × g, 10 min, 4°C; 5804R, Eppendorf), and the recovered supernatant was filtered (0.45 µm). The filtrate was passed through 10 kDa cut-off tubes, and the recovered filtrate was lyophilized and stored at -20°C until further use. The yield and DH were determined as described in Section 2.4.1.

2.5 | Electrophoretic profile

The albumin fraction and hydrolysates were separated by SDS-PAGE according to Laemmli (1970). The samples (15 µg) were mixed with a loading buffer and separated using a 12.5% polyacrylamide gel at 100 V with a SG-170 electrophoresis system (CBS Scientific, San Diego, CA, USA). The gel was stained with Coomassie Blue R250 (Sigma-Aldrich) and destained with a methanol: water: acetic acid solution (40:50:10). The image was acquired with a Chemidoc XRS system (BioRad, Hercules, CA, USA).

2.6 | Peptide profile of hydrolysates

The alcalase and pepsin-pancreatin hydrolysates were resuspended in HPLC-grade water (pH 8.0; 150 mg/mL). For analysis, 15 µL of the samples were injected into an ACCELA UPLC-DAD system (Thermo Scientific, San Jose, CA, USA) and separated using a Luna C18 column (150 × 4.6 mm × 5 µm; Phenomenex, Inc, Torrance, CA, USA). The mobile phases used were water containing 1% formic acid (A) and acetonitrile (B) at a flow rate of 0.2 mL/min with the following gradient: 0–20 min, 95.5%–96% A; 20–68 min, 96%–80% A; 68–115 min, 80%–52% A; 115–120 min, 52%–100% A. Detection was performed at 257 and 280 nm.

Peptides were identified with an LTQ-XL mass spectrometer (Thermo Scientific) equipped with an electrospray ionization source operating in positive mode. The capillary was set at 35 V and 300°C. Mass spectra acquisition ($m/z = 50$ –2000) was carried out with the Xcalibur 2.1 program (Thermo Scientific). Selected ions were fragmented by collision-induced dissociation. Data were analyzed with Proteome Discoverer 1.2 software using the SEQUEST algorithm and a referenced database (UNIPROT, *C. arietinum* proteome, ID: UP000087171). Cysteine carbamidomethylation and methionine oxidation were selected as variable modifications, while precursor and fragment mass tolerances were set to 10 ppm and 0.5 Da, respectively. The predicted biological activities of the identified peptides were explored using the BIOPEP-UWM database (Minkiewicz et al., 2008).

They were attributed to the whole peptide or a fragment thereof.

2.7 | In vitro AoxA

The in vitro AoxA was evaluated using two methods: ABTS assay (Re et al., 1999), and DPPH assay (Brand-Williams et al., 1995). The results were expressed as micromoles of Trolox equivalents (TE) per gram of hydrolysate ($\mu\text{mol TE/g H}$). For the ABTS assay, the hydrolysates were resuspended in phosphate-buffered saline (PBS, 1 mg/mL) and 20 μL were mixed with 180 μL of the radical solution (Abs 734 nm = 0.7 ± 0.1) in a 96-well microplate. The mixtures were allowed to react for 10 min at room temperature in the dark. The change in absorbance at 734 nm with respect to the reference (PBS) was registered using a Multiskan Sky microplate reader (Thermo Fisher, Waltham, MA, USA). In the DPPH assay, a radical solution was prepared in methanol (100 μM) and 100 μL were mixed with 100 μL of each hydrolysate (5 mg/mL) in a 96-well microplate. The mixture was incubated for 30 min at 37°C and then the absorbance was measured at 520 nm with a Multiskan Sky microplate reader (Thermo Fisher).

2.8 | In vivo AoxA

The AoxA was evaluated in 6-week-old male BALB-c mice (25–30 g). The animals were divided into five groups ($n = 6$), and the treatments were assigned as follows: group A, control receiving physiological saline solution (SS; 8 mL/kg BW); group B, acetaminophen (APAP) control receiving SS (8 mL/kg BW); group C, positive control receiving silymarin (100 mg/kg BW); group D, receiving alcalase CAH (100 mg/kg BW); and group E, receiving pepsin-pancreatin CAH (100 mg/kg BW). The doses were administered intragastrically once daily for 7 days (Papackova et al., 2018). On the seventh day, mice were fasted for 2 h before administering the last dose. Two hours later, mice in groups B–E were injected intraperitoneally with the oxidant APAP (350 mg/kg BW, 300 mg/10 mL H_2O at 55°C) to induce liver damage. In contrast, the non-damaged group (A) received an intraperitoneal injection of SS (10 mL/kg BW). After the APAP injection, mice had unrestricted access to water and food. Twenty-four hours after APAP application, followed by 16 h of fasting, blood samples were collected via cardiac puncture, and mice were dissected to obtain the liver. The blood was centrifuged at $4000 \times g$ for 10 min (5804R, Eppendorf). The recovered serum was collected to measure alkaline phosphatase using a commercial kit (Pointe Scientific Inc, Canton, MI, USA) following the manufacturer's instruc-

tions. The liver was weighed and divided into two parts, one was placed in 37% formalin for subsequent histopathological analysis, and the other was frozen at -70°C to determine the content of MDA and glutathione (GSH).

2.8.1 | MDA content

The concentration of MDA was determined using a colorimetric/fluorometric lipid peroxidation assay kit (Catalog K739-100, BioVision, Waltham, MA, USA). This assay is based on the reaction of MDA with thiobarbituric acid (TBA) to form an MDA-TBA adduct that is quantified at 532 nm.

For the analysis, 50 mg of liver tissue was homogenized in a microtube containing 150 μL of cold MDA lysis buffer and 1X butylated hydroxytoluene (BHT). The homogenate was centrifuged ($13,000 \times g$ / 10 min; 5410, Eppendorf), and the supernatant was recovered. A standard curve was prepared for quantification using dilutions from 0 to 30 nmol/well. A 100- μL aliquot of supernatant or standard dilution was mixed with 300 μL of TBA in 1.5 mL tubes to generate the MDA-TBA adduct. The tubes were incubated at 95°C for 60 min and then cooled on ice for 10 min. The mixture was centrifuged ($13,000 \times g$ / 3 min), and the supernatant was recovered. A 100- μL aliquot of each sample was placed in a 96-well flat-bottom microplate, and the absorbance was immediately measured at 532 nm using a Synergy HTX microplate reader (BioTek, Winooski, VT, USA). The results were expressed as nanomoles of MDA per milligram of liver tissue (nmol/mg) and calculated as follows: $\text{MDA (nmol/mg)} = (\text{A/mg}) * 4 * \text{D}$, where A is the amount of MDA (nmol) calculated from the standard curve, 4 is a correction factor, and D is the dilution factor if applicable.

2.8.2 | GSH content

GSH was quantified using a commercial kit (CS0260-1KT, Sigma-Aldrich). A liver sample (100 mg) was mixed with 500 μL of 5% sulfosalicylic acid (SSA) and homogenized in a microtube kept on ice. The sample was maintained cold for 10 min and centrifuged ($10,000 \times g$, 4°C, 10 min). The recovered supernatant was diluted 20 times (1:20) with 5% SSA. For quantification, a GSH calibration curve was prepared (3.125–100 μM). A 10- μL aliquot of the diluted sample or standard was mixed with 150 μL of the working mixture (5,5'-dithiobis (2-nitrobenzoic acid) [DTNB] + GSH reductase + buffer) and added to a microplate. The mixture was allowed to stand for 5 min at room temperature in the dark, then added with 50 μL of nicotinamide adenine dinucleotide phosphate (NADPH) and allowed to stand again

for 5 min at room temperature in the dark. The absorbance was measured at 412 nm using a Synergy HTX microplate reader (BioTek). The concentration of GSH concentration was expressed as nmol GSH/mg liver tissue.

2.8.3 | Histopathological analysis

For sample preparation, liver fragments were fixed in formalin buffered solution: 37% formaldehyde, 100 mL/L; sodium dihydrogen phosphate monohydrate ($\text{NaH}_2\text{PO}_4 \cdot \text{H}_2\text{O}$), 4 g/L; sodium hydrogen phosphate (Na_2HPO_4), 6.5 g/L, pH = 7.4. Tissue samples were cut (0.5 × 2.0 cm), dehydrated, and embedded in kerosene (Paraplast, Leica Biosystems, Deer Park, IL, USA). Sections with a thickness of 5–7 μm were then obtained with an RM2125 RTS microtome (Leica Biosystems). They were placed on slides and stained with hematoxylin–eosin. For preservation, the stained samples were sealed with a mounting medium (Entellan™ new, Merck, Darmstadt, Germany). The histological observations were performed under a Primo Star optical microscope (Carl Zeiss, Oberkochen, Germany) at magnifications of 10X and 40X. Photographs of representative slides were captured for further analysis.

2.9 | In vivo anti-inflammatory activity

The croton oil-induced ear edema method described by Mayhuasca et al. (2007) with the modifications of González Guevara et al. (2007) was used. Male BALB-c mice (28–40 g) were divided into four experimental groups ($n = 6$): group I, inflammation control (vehicle); group II, positive control (indomethacin, 500 $\mu\text{g}/\text{ear}$); groups III and IV, alcalase and pepsin-pancreatin CAH treatments (2000 $\mu\text{g}/\text{ear}$), respectively. The irritant, positive control, and treatments were dissolved in ethanol–water (1:1 v/v).

Each mouse received 20 μL of 5% croton oil and two applications of 10 μL on each surface (inner and outer) of the right pinna. The left (untreated) ear received just the vehicle. After inducing the edema, the positive control indomethacin (500 $\mu\text{g}/\text{ear}$) and CAH (2000 $\mu\text{g}/\text{ear}$) were administered topically (10 μL on each surface of the right pinna). After 4 h, the animals were euthanized by cervical dislocation, and 6-mm-diameter biopsies were obtained from each pinna. The extent of edema was calculated as the difference in weight between untreated and treated ears. The results were also expressed as edema-inhibition percentage with the equation:

$$\% \text{ inhibition} = \left[100 - \left(\frac{\text{Group edema treated}}{\text{Control group}} \right) \right] * 100.$$

Based on the edema % inhibition, the anti-inflammatory effect was classified as moderate (30%–65%) or good (> 65%; González Guevara et al., 2007).

2.10 | Hypoglycemic and anti-hyperglycemic activity

2.10.1 | Inhibition of α -glucosidase

It was determined as described by López-Angulo et al. (2019). Fifty microliters of CAH (100 mg/mL) and 100 μL of α -glucosidase solution (1 U/mL) were mixed and incubated for 10 min at 25°C. The mixture was added with 50 μL of *p*-nitrophenyl- α -D-glucopyranoside (5 mM) and incubated for 10 min, followed by measurement of the absorbance at 405 nm. Acarbose was used as a positive control (1.5 mg/mL). The results were expressed as percent inhibition and calculated as follows: $100 * [1 - (\text{Abs of sample}/\text{Abs of control})]$; where the control includes PBS, enzyme and *p*-nitrophenyl- α -D-glucopyranoside.

2.10.2 | Hypoglycemic activity

It was evaluated in normoglycemic male BALB-c mice according to Kifle et al. (2020) with some modifications. Four groups ($n = 6$) were formed: group I, negative control (saline); group II, positive control (glibenclamide 10 mg/kg BW); group III, alcalase CAH (100 mg/kg BW); group IV, pepsin-pancreatin CAH (100 mg/kg BW). The basal glucose level was measured after 4 h of fasting, and immediately afterward the treatments were administered orally, followed by measurement of the glucose levels every hour for 5 h. Blood was obtained by tail puncture and its glucose level (mg/dL) was measured with a glucometer (Accu-Chek® Roche, CDMX, Mexico).

2.10.3 | Anti-hyperglycemic activity

The oral glucose tolerance test was performed as described by Mohamed Sham Shihabudeen et al. (2011) with some modifications. Four groups ($n = 6$) of BALB-c mice were formed: group I, negative control (saline); group II, positive control (acarbose 10 mg/kg BW); group III, alcalase CAH (200 mg/kg BW); group IV, pepsin-pancreatin CAH (200 mg/kg BW). The basal glucose level was measured after 6 h of fasting, and immediately afterward the treatments were administered orally. Half an hour later, mice received sucrose (2 g/kg BW), and the glucose levels were measured after 30, 60, 90, and 120 min. Blood was

obtained by tail puncture and its glucose level (mg/dL) was measured with a glucometer (Accu-Chek®).

2.11 | Statistical analysis

All data were expressed as the mean and standard deviation. One-way ANOVA was used to analyze the antioxidant and anti-inflammatory activity data using Minitab 19 (Minitab Inc, State College, PA, USA). A repeated measures ANOVA was used to analyze hypoglycemic and anti-hyperglycemic activities using Statgraphics Plus 5.1 (StatPoint Technologies, Inc., Warrenton, VA, USA). Mean comparisons were evaluated using the Fisher's test ($P \leq 0.05$).

3 | RESULTS AND DISCUSSION

3.1 | DH and yield of the hydrolysates

Treatment of the chickpea albumin fraction with alcalase for 180 min resulted in a DH of 19.95%, while digestion of this fraction with pepsin-pancreatin achieved a DH of 50.2% (Figure 1a). These differences can be attributed to the type of enzyme used. Alcalase is an endopeptidase, while pancreatin is a mixture of endo- and exopeptidases that cleave hydrophobic and basic amino acids. The DH results are similar to those reported by Xu et al. (2020) for chickpea proteins hydrolyzed with alcalase (25.1%) and sequentially with alcalase-flavourzyme (50.2%). In agreement with the DH results, the yields obtained for the alcalase and pepsin-pancreatin CAH were 70.5% and 86.5%, respectively. These values correspond with the yield obtained for chickpea sprouted protein treated with alcalase (78%; Wali et al., 2021)

3.2 | Hydrolysates profiles

The SDS-PAGE analysis of the albumin fraction and its hydrolysates is shown in Figure 1b. The albumins exhibited several bands with a MW ranging from about 9 to 100 kDa (lane 2). This profile is similar to that reported by Clemente et al. (2000), who identified the low MW proteins (10 and 12 kDa) and the band of 23 kDa as albumins, while the band with the highest MW (92 kDa) may correspond to lipoxygenase (Figure 1b). Alcalase efficiently hydrolyzed the high MW proteins resulting in a continuous range of fragments from about 7 to 20 kDa (lane 3). Pepsin-pancreatin generated abundant fragments in the range of 10 to 13 kDa (lane 5). However, the hydrolysates filtered with 10 kDa cut-off tubes did not show visible protein bands (lanes 4 and 6).

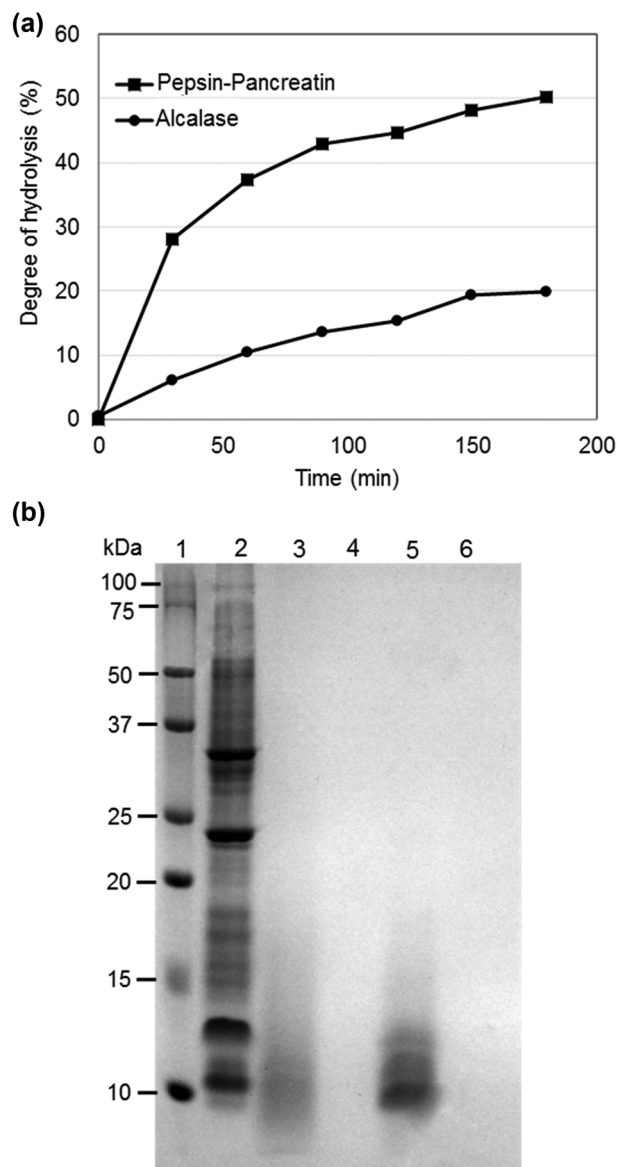


FIGURE 1 Degree of hydrolysis (DH) and electrophoretic profile of chickpea albumin hydrolysates (CAH). (a) DH (%) of alcalase CAH and pepsin-pancreatin CAH. (b) SDS-PAGE analysis of the albumin fraction and its hydrolysates. Lane 1, MW marker (kDa); lane 2, albumin fraction; lane 3, alcalase CAH; lane 4, alcalase CAH (≤ 10 kDa), lane 5, pepsin-pancreatin CAH; lane 6, pepsin-pancreatin CAH (≤ 10 kDa).

Xu et al. (2020) reported similar results for a chickpea alcalase hydrolysate.

The UPLC analysis showed 27 peaks for alcalase CAH and 28 for pepsin-pancreatin CAH (Figure S1). Each peak comprised multiple peptides, identifying in total 541 peptides in the alcalase CAH and 609 peptides in the pepsin-pancreatin CAH (Table S1). The differences in the number of peptides identified in the CAH were consistent with the DH (Figure 1). Most of the peptides identified have

TABLE 1 In vitro antioxidant activity of chickpea albumin hydrolysates (CAH) obtained using alcalase and pepsin-pancreatin.

Hydrolysate	ABTS % Inhibition ($\mu\text{mol ET/g H}$)	DPPH % Inhibition ($\mu\text{mol ET/g H}$)
Alcalase	64.8 ± 0.07^a (173.3 ± 0.21)	48.0 ± 1.64^a (24.9 ± 0.88)
Pepsin-pancreatin	64.9 ± 0.44^a (173.7 ± 1.18)	31.1 ± 0.90^b (15.0 ± 0.48)

Note: Hydrolysates were evaluated at 1 and 5 mg soluble protein/mL by ABTS and DPPH, respectively. Different letters in the same column indicate significant differences by the Fisher's test ($p \leq 0.05$). LSD ABTS = 0.72 (1.93) and LSD DPPH = 2.29 (1.23).

Abbreviations: ABTS, 2,2'-azino-bis(3-ethylbenzothiazolin)-6-sulfonic acid; DPPH, 2,2-diphenyl-1-picrylhydrazyl.

important predicted biological activities, highlighting the inhibitory activity against ACE and DPP4 (Table S1).

3.3 | In vitro AoxA

The AoxA by ABTS of both CAH was not significantly different (Table 1), even though the pepsin-pancreatin CAH showed a higher DH. However, the AoxA by DPPH was significantly higher in the alcalase CAH (48.0%), compared with the pepsin-pancreatin CAH (31.1%; Table 1). The number of low MW peptides with proton donor/acceptor amino acids (e.g., Lys) in the alcalase CAH was higher than in the pepsin-pancreatin CAH (Table S1), favoring its DPPH radical scavenging activity. The AoxA values obtained for ABTS were higher than those reported by Quintero-Soto et al. (2021; 41.5%, alcalase) and Sánchez-Chino et al. (2018; 24.8%, pepsin-pancreatin). On the contrary, the DPPH values were lower than those reported by Quintero-Soto et al. (2021) and Kou et al. (2013). The variations in AoxA could be attributed to differences in the protein extraction methods, the genotype, or the growing conditions. These results demonstrate that the use of enzymes with different sites of action can generate a variety of peptides with different activities, which may act alone or synergistically.

3.4 | In vivo AoxA

The alkaline phosphatase activity was similar among mice in the non-damaged (control), silymarin, and both CAH groups; these activity values were significantly lower than those observed in mice from the damaged group (APAP; $p \leq 0.05$; Figure 2a). Mice treated only with APAP showed significantly higher activity values than the control group ($p \leq 0.05$), indicating liver damage caused by APAP. These results agree with those reported by Kawakami et al. (2017a), who evaluated the protective effects of a sake lees hydrolysate against paracetamol-induced hepatotoxicity in ICR mice treated orally for seven days. In addition, Athira et al. (2013) investigated the protective effect of whey protein hydrolysate against hepato-nephrotoxicity induced by paracetamol (300 mg/kg BW) in mice, where the hydrolysate prevented the increase of hepatic markers,

including alkaline phosphatase. Based on these results, the CAH prepared with alcalase and pepsin-pancreatin in the present study showed hepatoprotective properties and may have potential applications in the prevention and treatment of oxidative stress-related diseases.

The hepatic MDA levels in mice treated with the pepsin-pancreatin CAH were similar to those treated with silymarin and the non-damaged control group. The MDA values of these three groups were significantly lower than that of the damaged group (APAP; $p \leq 0.05$). However, mice treated with the alcalase CAH did not show significant differences in MDA content, compared to the APAP group (Figure 2b). MDA is an end product of lipid peroxidation and a well-known biomarker of oxidative stress. The results obtained with the pepsin-pancreatin CAH are comparable to those reported using whey protein hydrolysates in mice (Athira et al., 2013); the authors observed a significant increase of MDA levels in the group treated with paracetamol, compared to the control group, while the group treated with the hydrolysate showed a decrease in the MDA content to normal levels. Dehiba et al. (2021) showed that a chickpea protein hydrolysate (1 g/kg BW) reduced the serum MDA levels in cholesterol-fed rats and provided protection against oxidative stress.

In the case of GSH, mice in the treated (silymarin and both CAH) and control groups had significantly higher values than those in the damaged group (APAP; $p \leq 0.05$; Figure 2c). Moreover, mice treated with the pepsin-pancreatin CAH and the reference drug silymarin showed higher GSH levels than those in the non-damaged control group. APAP-induced hepatotoxicity in rodents and humans is mediated by its reactive metabolite *N*-acetyl-*p*-benzoquinone imine (NAPQI). GSH forms adduct with APAP and contribute to the elimination of NAPQI, playing a crucial role in the antioxidant defense system and the prevention of APAP hepatotoxicity (Du et al., 2016; Vairetti et al., 2021). Kawakami et al. (2017a, 2017b) evaluated the effect of peptides from sake lees and rice on acetaminophen-induced hepatotoxicity in ICR mice. The animals were treated orally with the peptides (100 or 500 mg/kg BW) for 7 days and then injected intraperitoneally with acetaminophen (700 mg/kg BW) to induce hepatotoxicity. Pretreatment with the hydrolysates significantly restored the GSH levels reduced by the APAP

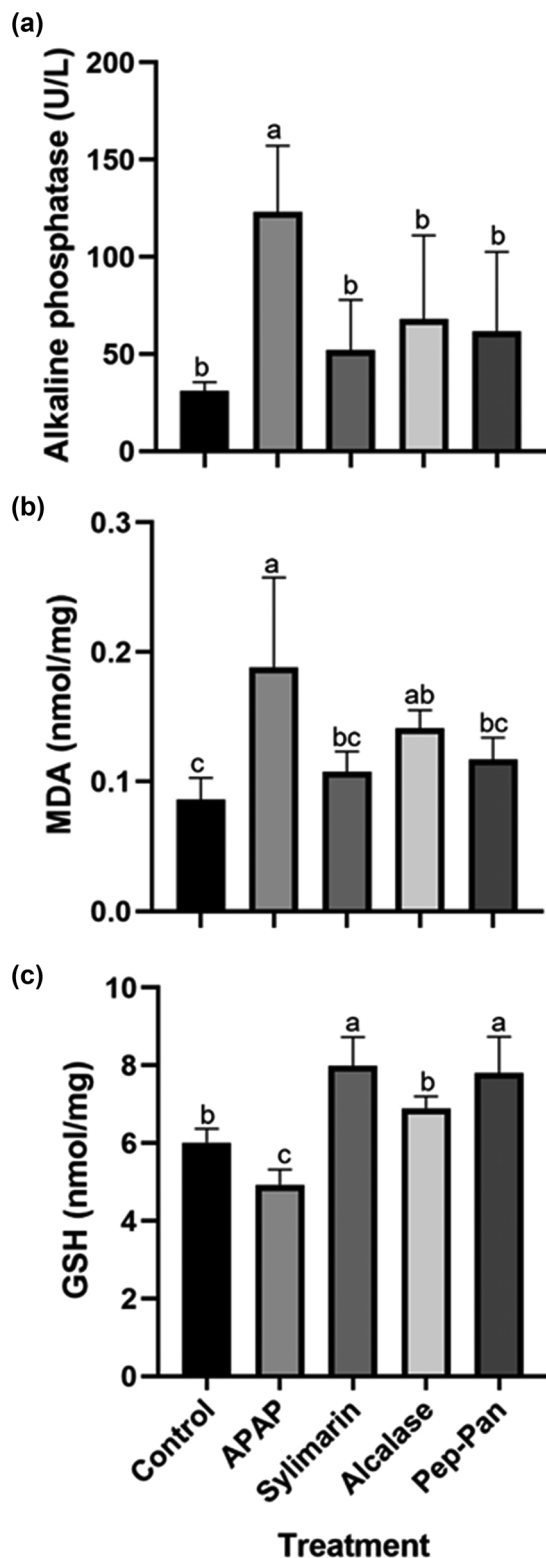


FIGURE 2 Effect of oral administration of CAH on serum alkaline phosphatase levels (a) and liver content of the oxidative stress markers malondialdehyde (MDA) (b) and glutathione (GSH) (c) in BALB-c mice with induced acute hepatotoxic damage. Treatments with alcalase CAH and pepsin-pancreatin CAH (100 mg/kg) were administered for 7 days. Liver damage was induced with *N*-acetyl-*p*-aminophenol (APAP) (350 mg/kg).

(Continues)

FIGURE 2 (Continued)

Non-damaged group (control). The results are expressed as the mean \pm SD ($n = 6$). Different letters indicate significant differences between treatments by the Fisher's test ($p \leq 0.05$). LSD AP = 49.6, LSD MDA = 0.05, LSD GSH = 0.90.

treatment. Therefore, the treatment of mice with alcalase and pepsin-pancreatin CAH protected the liver from GSH depletion (Figure 2c).

Based on the above results, the evaluated CAHs could act as detoxifying agents by increasing the intracellular antioxidant potential or GSH availability in the liver, which is important for protecting or treating hepatic injury. The antioxidant potential of the CAHs could be related to the number, molecular size, and amino acid composition of the peptides. The AoxA of the peptides appears to increase in the presence of hydrophobic amino acid residues such as valine or leucine at the amino-terminal end, as well as proline, histidine, tryptophan, tyrosine, methionine, and cysteine in their sequences (Karami & Akbari-Adergani, 2019). The different effects observed with the CAH may be associated with the number of peptides and the frequency of amino acids with potential AoxA: alcalase (541 peptides; Phe = 100, His = 32, Trp = 22, Pro = 161) and pepsin-pancreatin (609 peptides; Phe = 128, His = 56, Trp = 41, Pro = 191; Table S1).

3.5 | Histopathological evaluation

The liver histology of mice in the control group showed normal structures, including the central vein, hepatocytes, and sinusoids (Figure 3a,b). In contrast, severe structural changes were observed in the liver of the damaged group, characterized by the loose arrangement of hepatocytes, blood extravasation, necrosis, and damage to centrilobular cells with active inflammation (Figure 3c,d). The group treated with silymarin did not show relevant changes in liver structure (Figure 3e,f), while mice treated with the alcalase CAH showed less damage than those treated with APAP, exhibiting moderate centrilobular cell damage with inflammatory cell infiltration and blood extravasation (Figure 3g,h). Mice treated with pepsin-pancreatin CAH showed fewer pathological changes than the alcalase CAH-treated group, but the normal histological structure of the liver was not completely preserved (Figure 3i,j). These results correspond to those reported for hydrolysates from sake lees and rice (Kawakami et al., 2017a, 2017b), where the liver histological examinations of control and hydrolysate-treated mice showed normal lobular architecture and cellular structure. In contrast, APAP-treated mice (control damage) exhibited extensive areas of hepatic

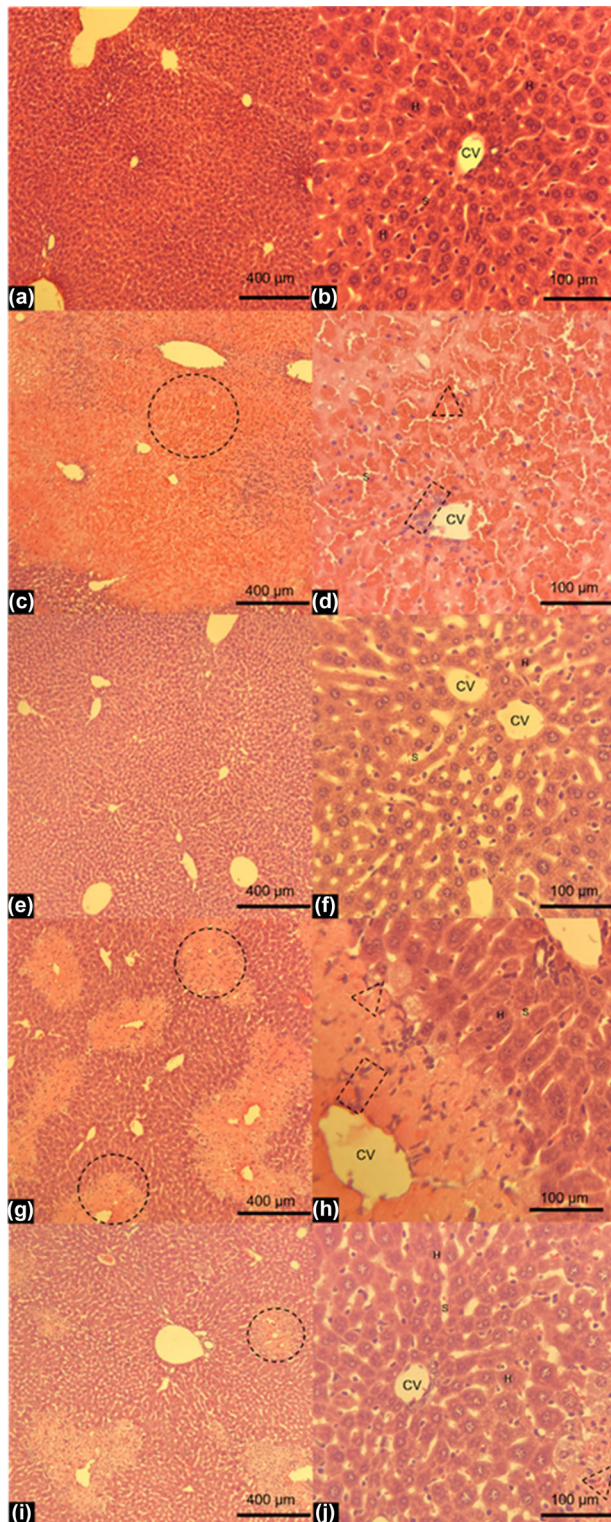


FIGURE 3 Effect of oral administration of CAH on liver morphology of BALB-c mice with acute acetaminophen-induced hepatotoxic damage (APAP) at 350 mg/kg (hematoxylin and eosin staining). Non-damaged control group (a and b), damaged group (c and d), silymarin group (e and f), alcalase group (g and h), pepsin-pancreatin group (i and j). CV, central vein; H, hepatocytes; S, sinusoids; circle, necrosis; triangle, blood extravasation; rectangle, inflammatory infiltrate.

TABLE 2 Anti-inflammatory activity of CAH in croton oil-induced mice ear edema.

Treatment	Edema (mg)	Inhibition (%)
Control	11.16 ± 1.27 ^a	0.00 ± 0.00 ^d
Indomethacin (500 μg/ear)	0.92 ± 0.41 ^d	91.76 ± 3.72 ^a
Alcalase CAH (2000 μg/ear)	3.56 ± 0.29 ^c	68.10 ± 2.58 ^b
Pepsin-pancreatin CAH (2000 μg/ear)	7.32 ± 1.15 ^b	34.40 ± 10.28 ^c

Note: The results are expressed as the mean ± SD ($n = 6$). Different letters in the same column indicate significant differences by the Fisher's test ($p \leq 0.05$). LSD Edema = 1.19 and LSD Inhibition = 7.53.

portal inflammation and hepatocellular necrosis, as well as a moderate increase in inflammatory cell infiltration. However, pretreatment with the hydrolysates mitigated these pathological changes. The results indicate that the CAH provided protection against APAP-induced liver injury.

3.6 | In vivo anti-inflammatory activity

The treatment with alcalase and pepsin-pancreatin CAH reduced the inflammation in mice ears (Table 2). The anti-inflammatory effect was good with the alcalase CAH (68.1%) and moderate with pepsin-pancreatin CAH (34.4%; González Guevara et al., 2007).

The inflammation caused by croton oil is mainly due to the irritant 12-*O*-tetradecanoylphorbol-13-acetate, which activates protein kinase C that stimulates the release of proinflammatory cytokines and other mediators such as phospholipase and arachidonic acid. These mechanisms lead to increased vascular permeability, vasodilation, and swelling due to the release of histamine and serotonin, followed by the synthesis of leukotrienes and prostaglandins. Therefore, anti-inflammatory drugs or supplements that inhibit these mechanisms effectively suppress croton oil-induced ear edema (Sangchart et al., 2021).

Clementi et al. (1995) evaluated the anti-inflammatory activity of two peptides (amylin and calcytokinin gene-related peptide [CGRP]) on croton oil-induced mouse ear edema. CGRP showed 68% inhibition of ear edema at 0.02 μg/ear and was more potent than amylin which exhibited 62% inhibition at a higher concentration (10 μg/ear).

3.7 | Inhibition of α -glucosidase activity

Alcalase CAH (100 mg/mL) and pepsin-pancreatin CAH (100 mg/mL) showed 31.1% and 52.4% inhibition of the α -glucosidase activity, respectively. Acevedo-Martínez & Gonzalez de Mejia (2021) reported lower inhibition

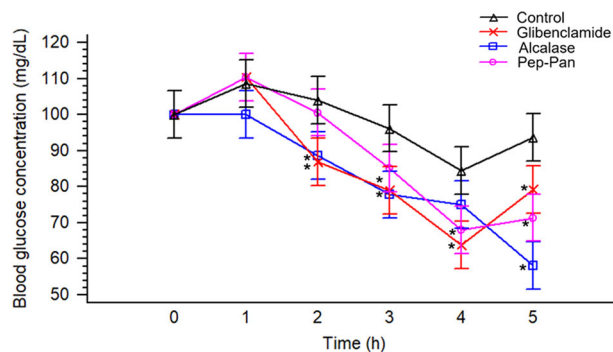


FIGURE 4 Hypoglycemic effect of CAH (100 mg/kg body weight [BW]) obtained with alcalase and pepsin-pancreatin in normoglycemic mice. Glibenclamide was used as a positive control (10 mg/kg BW). Data are expressed as the mean \pm standard error ($n = 6$). *Indicates significant difference with respect to the negative control (Fisher, $p \leq 0.05$). LSD = 13.13.

values (1%–17%) of α -glucosidase for pepsin-pancreatin hydrolysates (10 mg/mL) derived from five chickpea varieties. Also, the percent inhibition of α -glucosidase obtained for the alcalase hydrolysate was lower than the 43.8% reported previously by Quintero-Soto et al. (2021). These discrepancies could be attributed to variations in protein extraction methodology, growing conditions, and the genotype. Nevertheless, the results suggested the potential α -glucosidase inhibitory activity of the hydrolysates in vivo, so their hypoglycemic and anti-hyperglycemic activity was evaluated in vivo in BALB-c mice.

3.8 | Hypoglycemic activity

The basal glucose levels of the experimental groups (122 ± 12.3 mg/dL) were within the reported normal range (75–128 mg/dL; Santos et al., 2016). The glucose concentration in normoglycemic BALB-c mice treated with both alcalase CAH and pepsin-pancreatin CAH (100 mg/kg BW) showed a gradual decrease, reaching similar values to those obtained with the control group treated with glibenclamide (10 mg/kg BW; Figure 4). The alcalase CAH was more effective in reducing the glucose levels, showing a significantly lower concentration than the control group 2 h after the dose administration and a similar value to that obtained with glibenclamide (Figure 4). This contrast with the hypoglycemic peak observed in animals 1 h after insulin administration, where the recovery of the basal glucose levels is slow (Valencia-Mejía et al., 2019). The hypoglycemic pattern observed in mice treated with CAH was similar to that of normoglycemic Wistar rats treated with bean protein hydrolysates (Valencia-Mejía et al., 2019). These results suggest that the CAH improved

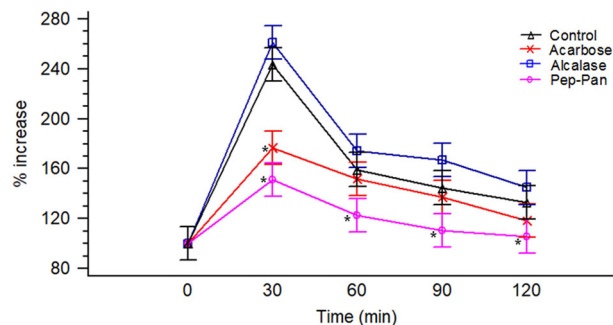


FIGURE 5 Anti-hyperglycemic effect of CAH (200 mg/kg BW) obtained with alcalase and pepsin-pancreatin in normoglycemic mice after sucrose administration. Acarbose was used as a positive control (10 mg/kg BW). Data are expressed as the mean \pm standard error ($n = 6$). *Indicates significant difference with respect to the negative control (Fisher, $p \leq 0.05$). LSD = 26.74.

the ability of the tissues to absorb or metabolize glucose without inducing a hypoglycemic peak. Both CAHs may share a common hypoglycemic mechanism associated with increased insulin release or enhancement of the insulin signaling cascade. The hypoglycemic effect of the CAHs could involve the phosphatidylinositol-3-kinase (PI3K) pathway, the main mechanism used by insulin to regulate glucose and lipid metabolism. In addition, the adenosine monophosphate-dependent protein kinase (AMPK) pathway improves glucose uptake by increasing GLUT4 expression and its translocation to the membrane in skeletal muscle, therefore the AMPK pathway is also relevant for the prevention and treatment of diabetes (Coughlan et al., 2014; Gutiérrez-Rodelo et al., 2017). However, additional biochemical and molecular studies are required to elucidate the specific pathways involved in the hypoglycemic effect of the CAH.

3.9 | Anti-hyperglycemic activity

The basal glucose levels of the experimental groups (108 ± 28.8 mg/dL) were within the reported normal range (75–128 mg/dL; Santos et al., 2016). Normoglycemic mice treated with pepsin-pancreatin CAH and acarbose showed a similar anti-hyperglycemic pattern, significantly reducing the hyperglycemic peak observed 30 min after sucrose loading (Figure 5). At this time point, the average increase in glucose levels was 143.5% for the control group, which was similar ($p > 0.05$) to that observed for the alcalase CAH group (149.2%). In contrast, the increase in glucose levels was significantly ($p \leq 0.05$) reduced in the pepsin-pancreatin CAH group (51.1%), and this value was lower than that obtained with the positive control acarbose at 10 mg/kg (76.5%; Figure 5). The alcalase CAH did not

show an anti-hyperglycemic activity since the glucose variation pattern in the treated mice over time was similar to that of the control group (Figure 5). On the other hand, the pepsin-pancreatin CAH showed anti-hyperglycemic activity, suggesting its potential use as an antidiabetic agent.

The glucose tolerance test mimics blood glucose levels in a postprandial state and provides valuable information on anti-hyperglycemic activity. The results of this study are in agreement with those obtained by Valencia-Mejía et al. (2019), who used pepsin-pancreatin hydrolysates from beans in the oral starch tolerance test in Wistar rats. The authors demonstrated that the fractions evaluated showed similar or even better results than the positive control acarbose. Also, Nuñez-Aragón et al. (2019) evaluated the effect of six hydrolysates and six < 1 kDa fractions from *Phaseolus lunatus*, *P. vulgaris*, and *Mucuna pruriens* on the postprandial hyperglycemia in Wistar rats. Most treatments that showed significant activity were obtained using the pepsin-pancreatin hydrolysis system (five out of seven), whereas the alcalase-flavourzyme system produced only two active treatments. This difference can be attributed to the fact that pepsin-pancreatin hydrolysis simulates gastric digestion, and the active peptides obtained are retained after oral administration and absorbed by the epithelial cells in the small intestine. The results of the present study could be explained in the same way since pepsin-pancreatin CAH showed anti-hyperglycemic activity, while alcalase CAH did not. Additionally, the higher glucosidase inhibition obtained for the pepsin-pancreatin hydrolysate is consistent with its anti-hyperglycemic activity and may partially explain its mechanism of action.

4 | CONCLUSION

Chickpea albumins treated with alcalase and pepsin-pancreatin exhibited strong inhibitory activity against ABTS and DPPH radicals, as well as hepatoprotective effects, indicating their potential as antioxidants to control the oxidative stress. The hydrolysates also showed anti-inflammatory activity in croton-induced mouse edema, suggesting their potential to reduce inflammation. Furthermore, both hydrolysates showed hypoglycemic activity in vivo, but only the pepsin-pancreatin hydrolysate reduced the postprandial hyperglycemia, indicating its potential for the treatment of diabetes. Nevertheless, further studies using diabetic animal models are necessary to confirm and better understand the therapeutic effects of these hydrolysates in managing diabetes. Additionally, investigating the underlying mechanisms of action would provide valuable insights into how these hydrolysates exert their beneficial effects. Overall, the demonstrated in vivo

activities of chickpea hydrolysates suggest their potential use in treating chronic diseases associated with oxidative stress and inflammation.

AUTHOR CONTRIBUTIONS

Alicia Navarro-Leyva: Investigation; writing—original draft; methodology. **Gabriela López-Angulo:** Investigation; writing—original draft; methodology. **Francisco Delgado-Vargas:** Writing—review and editing; conceptualization. **José Ángel López-Valenzuela:** Conceptualization; writing—review and editing; supervision; funding acquisition.

ACKNOWLEDGMENTS

This work was supported by the Autonomous University of Sinaloa [PROFAPI, PRO-A7-021]. ANL received a scholarship from CONACYT-Mexico.

CONFLICT OF INTEREST STATEMENT

The authors declare they have no conflicts of interest.

ORCID

José Ángel López-Valenzuela  <https://orcid.org/0000-0002-9358-5030>

REFERENCES

- Acevedo-Martínez, K. A., & Gonzalez de Mejia, E. (2021). Comparison of five chickpea varieties, optimization of hydrolysates production and evaluation of biomarkers for type 2 diabetes. *Food Research International*, 147, 110572. <https://doi.org/10.1016/j.foodres.2021.110572>
- Adler-Nissen, J. (1979). Determination of the degree of hydrolysis of food protein hydrolysates by trinitrobenzenesulfonic acid. *Journal of Agricultural and Food Chemistry*, 27(6), 1256–1262. <https://doi.org/10.1021/jf60226a042>
- Athira, S., Mann, B., Sharma, R., & Kumar, R. (2013). Ameliorative potential of whey protein hydrolysate against paracetamol-induced oxidative stress. *Journal of Dairy Science*, 96(3), 1431–1437. <https://doi.org/10.3168/jds.2012-6080>
- Brand-Williams, W., Cuvelier, M. E., & Berset, C. (1995). Use of a free radical method to evaluate antioxidant activity. *LWT—Food Science and Technology*, 28(1), 25–30. [https://doi.org/10.1016/S0023-6438\(95\)80008-5](https://doi.org/10.1016/S0023-6438(95)80008-5)
- Brown, R. E., Jarvis, K. L., & Hyland, K. J. (1989). Protein measurement using bicinchoninic acid: Elimination of interfering substances. *Analytical Biochemistry*, 180(1), 136–139. [https://doi.org/10.1016/0003-2697\(89\)90101-2](https://doi.org/10.1016/0003-2697(89)90101-2)
- Chavez-Ontiveros, J., Quintero-Soto, M. F., Pineda-Hidalgo, K. V., Lopez-Moreno, H. S., Reyes Moreno, C., Garzon-Tiznado, J. A., & Lopez-Valenzuela, J. A. (2020). Microsatellite-based genetic diversity and grain quality variation in chickpea genotypes from Mexico and international collections. *Agrociencia*, 54, 57–73.
- Chavez-Ontiveros, J., Reyes-Moreno, C., Ramirez-Torres, G. I., Figueroa-Salcido, O. G., Aramburo-Galvez, J. G., Montoya-Rodríguez, A., Ontiveros, N., & Cuevas-Rodríguez, E. O. (2022). Extrusion improves the antihypertensive potential of a kabuli

- chickpea (*Cicer arietinum* L.) protein hydrolysate. *Foods*, 11(17), 2562. <https://doi.org/10.3390/foods11172562>
- Clemente, A., Vioque, J., Sánchez-Vioque, R., Pedroche, J., Bautista, J., & Millán, F. (2000). Factors affecting the in vitro protein digestibility of chickpea albumins. *Journal of the Science of Food and Agriculture*, 80(1), 79–84. [https://doi.org/10.1002/\(SICI\)1097-0010\(20000101\)80:1<79::AID-JSFA487>3.0.CO;2-4](https://doi.org/10.1002/(SICI)1097-0010(20000101)80:1<79::AID-JSFA487>3.0.CO;2-4)
- Clementi, G., Caruso, A., Maria Catena Cutuli, V., Prato, A., de Bernardis, E., Erio Fiore, C., & Amico-Roxas, M. (1995). Anti-inflammatory activity of amylin and CGRP in different experimental models of inflammation. *Life Sciences*, 57(14), 193–197. [https://doi.org/10.1016/0024-3205\(95\)02100-W](https://doi.org/10.1016/0024-3205(95)02100-W)
- Coughlan, K. A., Valentine, R. J., Ruderman, N. B., & Saha, A. K. (2014). AMPK activation: A therapeutic target for type 2 diabetes? *Diabetes, Metabolic Syndrome and Obesity: Targets and Therapy*, 7, 241–253. <https://doi.org/10.2147/dms0.S43731>
- Dehiba, F., Allaoui, A., Benomar, S., Yahia, S., Guillén, N., Rodríguez-Yoldi, M. J., Osada, J., & Boualga, A. (2021). Protective properties of sardine and chickpea protein hydrolysates against lipoprotein oxidative damages and some inflammation markers in hypercholesterolemic rats. *Mediterranean Journal of Nutrition and Metabolism*, 14, 439–452. <https://doi.org/10.3233/MNM-210548>
- Du, K., Ramachandran, A., & Jaeschke, H. (2016). Oxidative stress during acetaminophen hepatotoxicity: Sources, pathophysiological role and therapeutic potential. *Redox Biology*, 10, 148–156. <https://doi.org/10.1016/j.redox.2016.10.001>
- FAOSTAT. (2022). *Food and Agriculture Organization statistical database*. <http://faostat.fao.org>
- González Guevara, M., Lf, O., & J, C. (2007). Evaluación de extractos y fracciones de plantas colombianas en modelos de inflamación aguda, subaguda y crónica. *Revista Colombiana de Ciencias Químico-Farmacéuticas*, 36(2), 166–174.
- Gutiérrez-Rodelo, C., Roura-Guiberna, A., & Olivares-Reyes, J. (2017). Mecanismos moleculares de la resistencia a la insulina: Una actualización. *Gaceta Médica de México*, 153, 214–228.
- Karami, Z., & Akbari-Adergani, B. (2019). Bioactive food derived peptides: A review on correlation between structure of bioactive peptides and their functional properties. *Journal of Food Science and Technology*, 56(2), 535–547. <https://doi.org/10.1007/s13197-018-3549-4>
- Kawakami, K., Moritani, C., Uraji, M., Fujita, A., Kawakami, K., Hatanaka, T., Suzaki, E., & Tsuboi, S. (2017a). Sake lees hydrolysate protects against acetaminophen-induced hepatotoxicity via activation of the Nrf2 antioxidant pathway. *Journal of Clinical Biochemistry and Nutrition*, 61(3), 203–209. <https://doi.org/10.3164/jcfn.17-21>
- Kawakami, K., Moritani, C., Uraji, M., Fujita, A., Kawakami, K., Hatanaka, T., Suzaki, E., & Tsuboi, S. (2017b). Hepatoprotective effects of rice-derived peptides against acetaminophen-induced damage in mice. *Journal of Clinical Biochemistry and Nutrition*, 60(2), 115–120. <https://doi.org/10.3164/jcfn.16-44>
- Kifle, Z. D., Yesuf, J. S., & Atnafie, S. A. (2020). Evaluation of in vitro and in vivo anti-diabetic, anti-hyperlipidemic and anti-oxidant activity of flower crude extract and solvent fractions of *Hagenia abyssinica* (Rosaceae). *Journal of Experimental Pharmacology*, 12, 151–167. <https://doi.org/10.2147/JEP.S249964>
- Kou, X., Gao, J., Xue, Z., Zhang, Z., Wang, H., & Wang, X. (2013). Purification and identification of antioxidant peptides from chickpea (*Cicer arietinum* L.) albumin hydrolysates. *LWT—Food Science and Technology*, 50(2), 591–598. <https://doi.org/10.1016/j.lwt.2012.08.002>
- Laemmli, U. K. (1970). Cleavage of structural proteins during the assembly of the head of bacteriophage T4. *Nature*, 227(5259), 680–685. <https://doi.org/10.1038/227680a0>
- López-Angulo, G., Montes-Avila, J., Díaz-Camacho, S. P., Vega-Aviña, R., Ahumada-Santos, Y. P., & Delgado-Vargas, F. (2019). Chemical composition and antioxidant, α -glucosidase inhibitory and antibacterial activities of three *Echeveria* DC. species from Mexico. *Arabian Journal of Chemistry*, 12(8), 1964–1973. <https://doi.org/10.1016/j.arabjc.2014.11.050>
- Mayhuasca, O., Bonilla, P., Ballón, M., Ferreira, M., & Carrasco, E. (2007). Antiinflammatory effect in mice of extracts of *Calceolaria tripartita* R & P, compared phytochemical with the hydroalcoholic extract of *Calceolaria melissifolia* “Bentham”. *Ciencia e Investigación*, 10(2), 71–80. <https://doi.org/10.15381/ci.v10i2.5042>
- Milan-Noris, A. K., Gutierrez-Urbe, J. A., Santacruz, A., Serna-Saldívar, S. O., & Martínez-Villaluenga, C. (2018). Peptides and isoflavones in gastrointestinal digests contribute to the anti-inflammatory potential of cooked or germinated desi and kabuli chickpea (*Cicer arietinum* L.). *Food Chemistry*, 268, 66–76. <https://doi.org/10.1016/j.foodchem.2018.06.068>
- Minkiewicz, P., Dziuba, J., Iwaniak, A., Dziuba, M., & Darewicz, M. (2008). BIOPEP database and other programs for processing bioactive peptide sequences. *Journal of AOAC International*, 91(4), 965–980. <https://doi.org/10.1093/jaoac/91.4.965>
- Mohamed Sham Shihabudeen, H., Hansi Priscilla, D., & Thirumurugan, K. (2011). Cinnamon extract inhibits α -glucosidase activity and dampens postprandial glucose excursion in diabetic rats. *Nutrition & Metabolism*, 8(1), 46–46. <https://doi.org/10.1186/1743-7075-8-46>
- Mojica, L., Gonzalez de Mejia, E., Granados-Silvestre, M. Á., & Menjivar, M. (2017). Evaluation of the hypoglycemic potential of a black bean hydrolyzed protein isolate and its pure peptides using in silico, in vitro and in vivo approaches. *Journal of Functional Foods*, 31, 274–286. <https://doi.org/10.1016/j.jff.2017.02.006>
- Núñez-Aragón, P. N., Segura-Campos, M., Negrete-León, E., Acevedo-Fernández, J. J., Betancur-Ancona, D., Chel-Guerrero, L., & Castañeda-Corral, G. (2019). Protein hydrolysates and ultrafiltered < 1 kDa fractions from *Phaseolus lunatus*, *Phaseolus vulgaris* and *Mucuna pruriens* exhibit antihyperglycemic activity, intestinal glucose absorption and α -glucosidase inhibition with no acute toxicity in rodents. *Journal of the Science of Food and Agriculture*, 99(2), 587–595. <https://doi.org/10.1002/jsfa.9219>
- Ortiz-Martínez, M., Otero-Pappatheodorou, J. T., Serna-Saldívar, S. O., & García-Lara, S. (2017). Antioxidant activity and characterization of protein fractions and hydrolysates from normal and quality protein maize kernels. *Journal of Cereal Science*, 76, 85–91. <https://doi.org/10.1016/j.jcs.2017.05.021>
- Papackova, Z., Heczakova, M., Dankova, H., Sticova, E., Lodererova, A., Bartonova, L., Poruba, M., & Cahova, M. (2018). Silymarin prevents acetaminophen-induced hepatotoxicity in mice. *PLoS ONE*, 13(1), e0191353. <https://doi.org/10.1371/journal.pone.0191353>
- Quintero-Soto, M. F., Chávez-Ontiveros, J., Garzón-Tiznado, J. A., Salazar-Salas, N. Y., Pineda-Hidalgo, K. V., Delgado-Vargas, F., & López-Valenzuela, J. A. (2021). Characterization of peptides with antioxidant activity and antidiabetic potential obtained from chickpea (*Cicer arietinum* L.) protein hydrolysates. *Journal of Food Science*, 86, 2962–2977. <https://doi.org/10.1111/1750-3841.15778>

- Re, R., Pellegrini, N., Proteggente, A., Pannala, A., Yang, M., & Rice-Evans, C. (1999). Antioxidant activity applying an improved ABTS radical cation decolorization assay. *Free Radical Biology & Medicine*, 26(9-10), 1231–1237. [https://doi.org/10.1016/s0891-5849\(98\)00315-3](https://doi.org/10.1016/s0891-5849(98)00315-3)
- Sánchez-Chino, X. M., Jiménez-Martínez, C., León-Espinosa, E. B., Garduño-Siciliano, L., Álvarez-González, I., Madrigal-Bujaidar, E., Vásquez-Garzón, V. R., Baltiérrez-Hoyos, R., & Dávila-Ortiz, G. (2018). Protective effect of chickpea protein hydrolysates on colon carcinogenesis associated with a hypercaloric diet. *Journal of the American College of Nutrition*, 38(2), 162–170. <https://doi.org/10.1080/07315724.2018.1487809>
- Sangchart, P., Panyatip, P., Damrongrungruang, T., Pripem, A., Mahakunakorn, P., & Puthongking, P. (2021). Anti-inflammatory comparison of melatonin and its bromobenzoylamide derivatives in lipopolysaccharide (LPS)-induced RAW 264.7 cells and croton oil-induced mice ear edema. *Molecules (Basel, Switzerland)*, 26(14), 4285. <https://doi.org/10.3390/molecules26144285>
- Santos, E. W., Oliveira, D. C. d., Hastreiter, A., Silva, G. B. d., Beltran, J. S. d. O., Tsujita, M., Crisma, A. R., Neves, S. M. P., Fock, R. A., & Borelli, P. (2016). Hematological and biochemical reference values for C57BL/6, Swiss Webster and BALB/c mice. *Brazilian Journal of Veterinary Research and Animal Science*, 53(2), 138–145. <https://doi.org/10.11606/issn.1678-4456.v53i2p138-145>
- Vairetti, M., Di Pasqua, L. G., Cagna, M., Richelmi, P., Ferrigno, A., & Berardo, C. (2021). Changes in glutathione content in liver diseases: An update. *Antioxidants*, 10(3), 364. <https://doi.org/10.3390/antiox10030364>
- Valencia-Mejía, E., Batista, K. A., Fernández, J. J. A., & Fernandes, K. F. (2019). Antihyperglycemic and hypoglycemic activity of naturally occurring peptides and protein hydrolysates from easy-to-cook and hard-to-cook beans (*Phaseolus vulgaris* L.). *Food Research International*, 121, 238–246. <https://doi.org/10.1016/j.foodres.2019.03.043>
- Wali, A., Mijiti, Y., Yanhua, G., Yili, A., Aisa, H. A., & Kawuli, A. (2021). Isolation and identification of a novel antioxidant peptide from chickpea (*Cicer arietinum* L.) sprout protein hydrolysates. *International Journal of Peptide Research and Therapeutics*, 27(1), 219–227. <https://doi.org/10.1007/s10989-020-10070-2>
- Xu, Y., Galanopoulos, M., Sismour, E., Ren, S., Mersha, Z., Lynch, P., & Almutaimi, A. (2020). Effect of enzymatic hydrolysis using endo- and exo-proteases on secondary structure, functional, and antioxidant properties of chickpea protein hydrolysates. *Journal of Food Measurement and Characterization*, 14, 343–352. <https://doi.org/10.1007/s11694-019-00296-0>
- Xue, Z., Wen, H., Zhai, L., Yu, Y., Li, Y., Yu, W., Cheng, A., Wang, C., & Kou, X. (2015). Antioxidant activity and anti-proliferative effect of a bioactive peptide from chickpea (*Cicer arietinum* L.). *Food Research International*, 77, 75–81. <https://doi.org/10.1016/j.foodres.2015.09.027>

SUPPORTING INFORMATION

Additional supporting information can be found online in the Supporting Information section at the end of this article.

How to cite this article: Navarro-Leyva, A., López-Angulo, G., Delgado-Vargas, F., & López-Valenzuela, J. Á. (2023). Antioxidant, anti-inflammatory, hypoglycemic, and anti-hyperglycemic activity of chickpea protein hydrolysates evaluated in BALB-c mice. *Journal of Food Science*, 1–13. <https://doi.org/10.1111/1750-3841.16744>